Synthesis and Characterization of Vanadyl Hydrogen Phosphite Hydrate

Wen-Sheng Dong, Jonathan K. Bartley, Nian-Xue Song, and Graham J. Hutchings*

School of Chemistry, Cardiff University, Cardiff CF10 3AT, United Kingdom

Received December 21, 2004. Revised Manuscript Received March 4, 2005

A novel method for the preparation of vanadyl hydrogen phosphite hydrates is described. The reaction of V_2O_5, H_3PO_3, and 1-propanol in the absence of water at 150 °C led to the formation of $VOHPO_3 \cdot 1.5H_2O$ with high surface area (ca. 50 m^2/g), whereas in the presence of water $VOHPO_3 \cdot H_2O$ was the unique product. The materials were characterized using a combination of techniques including elemental analysis, thermogravimetric analysis, powder X-ray diffraction, laser Raman spectroscopy, and infrared spectroscopy. On heating the sample in flowing nitrogen at 750 °C, it was found that the vanadyl(IV) hydrogen phosphite(III) hydrates transformed into vanadium(III) phosphate(V), VPO_4, via an internal oxidation−reduction process between V(IV) and P(III), wherein V(IV) was reduced to V(III) and P(III) was oxidized to P(V). Whereas, heating the vanadyl hydrogen phosphite hydrates in flowing hydrogen can inhibit the phase transformation from vanadyl hydrogen phosphite to VPO_4. The catalytic performance for the selective oxidation of *n*-butane to maleic anhydride using the final catalysts prepared by in situ activation under the reaction conditions was contrasted. It was found that the catalyst derived from the $VOHPO_3 \cdot H_2O$ precursor shows a higher intrinsic activity for the production of maleic anhydride than that derived from $VOHPO_3 \cdot 1.5H_2O$.

Introduction

The discovery of vanadium−phosphorus−oxide systems, which are well-known as commercial catalysts for the partial oxidation of *n*-butane to maleic anhydride, has promoted extensive studies concerning the synthesis of new vanadium phosphate phases.[1−11] One main reason is that vanadium phosphates can be prepared as a large number of specific phases both due to the variable oxidation state of vanadium and the large number of ways in which vanadium−oxygen polyhedra (octahedra or square pyramids) and phosphate tetrahedra can be connected to form two- or three-dimensional networks.[1,2] To date, many well-characterized, crystalline vanadium phosphate phases have been identified whose structures and catalytic properties have been well documented. Some of the most widely studied are the V(V) vanadyl orthophosphates (α-, *β*-, *γ*-, *δ*-, and *ω*-$VOPO_4$ and $VOPO_4 \cdot 2H_2O$) and the V(IV) vanadyl hydrogen phosphates ($VOHPO_4 \cdot 2H_2O$, $VOHPO_4 \cdot 0.5H_2O$, $VO(H_2PO_4)_2$), vanadyl metaphosphate ($VO(PO_3)_2$), and vanadyl pyrophosphate ($(VO)_2P_2O_7$) which is claimed to be the active phase of commercial catalysts.[12−16]

Johnson and co-workers synthesized a series of layered V(IV)/P(III) compounds of general composition $VO(C_nH_{2n+1}PO_3) \cdot yH_2O$ ($y = 1.5$, $1 \le n \le 3$; $y = 1.0$, $4 \le n \le 8$) by hydrothermal reaction of V_2O_3 and corresponding alkylphosphonic acid in water at 200 °C.[3−5] The compounds with $n \le 3$ have structures similar to that of $VOHPO_4 \cdot 0.5H_2O$. The compositions with $4 \le n \le 8$ also are layered, with structures apparently related to that of $VO(C_6H_5PO_3) \cdot H_2O$. Subsequently, Guliants and co-workers reported the synthesis and characterization of vanadyl(IV) phosphite, $VOHPO_3 \cdot 1.5H_2O$, and vanadyl *n*-butylphosphonates, $VOC_4H_9PO_3 \cdot xH_2O$.[6−8] Worzala was the first to prepare vanadyl hydrogen phosphite monohydrate, $VOHPO_3 \cdot H_2O$, by heating an aqueous solution of $VO(H_2PO_3)_2$ at 120 °C for 12 h and determined the unit cell parameters of the compound by powder X-ray diffraction.[9]

In this study we describe a novel method for the preparation of vanadyl hydrogen phosphite hydrates and their

* To whom correspondence should be addressed. Phone: +44(0)29-20874023. Fax: +44(0)29-20874030. E-mail: hutch@cardiff.ac.uk.

(1) Johnson, J. W.; Johnston, D. C.; Jacobson, A. J.; Brody, J. F. *J. Am. Chem. Soc.* **1984**, *106*, 8123.
(2) Vaughey, J. T.; Harrison, W. T. A.; Jacobson, A. J. *Inorg. Chem.* **1994**, *33*, 2481.
(3) Huan, G.; Johnson, J. W.; Brody, J. F.; Goshorn, D. P. *Mater. Chem. Phy.* **1993**, *35*, 199.
(4) Huan, G.; Jacobson, A. J.; Johnson, J. W.; Corcoran, E. W. *Chem. Mater.* **1990**, *2*, 91.
(5) Huan, G.; Jacobson, A. J.; Johnson, J. W.; Goshorn, D. P. *Chem. Mater.* **1992**, *4*, 661.
(6) Guliants, V. V.; Benziger, J. B.; Sundaresan, S. *Chem. Mater.* **1995**, *7*, 1493.
(7) Guliants, V. V.; Benziger, J. B.; Sundaresan, S. *Chem. Mater.* **1995**, *7*, 1485.
(8) Guliants, V. V.; Benziger, J. B.; Sundaresan, S. *J. Catal.* **1995**, *156*, 298.
(9) Worzala, H. Inst. f. Angewandte Chemie e.V., Berlin, Germany, ICDD Grant-in-Aid (1996).
(10) Fratzky, D.; Gotze, Th.; Worzala, H.; Meisel, M. *Mater. Res. Bull.* **1998**, *33*, 635.
(11) Bartley, J. K.; Kiely, Ch. J. R.; Wells, P. K.; Hutchings, G. J. *Catal. Lett.* **2001**, *72*, 99.
(12) Bordes, E. *Catal. Today* **1987**, *1*, 499.
(13) Vanadyl Pyrophosphate Catalysts. *Catal. Today* **1993**, *16*, 1 (G. Centi, Ed.).
(14) Abdelouahab, F. B.; Olier, R.; Guilhaume, N.; Lefebvre, F.; Volta, J. C. *J. Catal.* **1992**, *134*, 151.
(15) Hutchings, G. J.; Sananes, M. T.; Sajip, S.; Kiely, Ch. J.; Burrows, A.; Ellison, I. J.; Volta, J. C. *Catal. Today* **1997**, *33*, 161.
(16) Guliants, V. V.; Benziger, J. B.; Sundaresan, S.; Wachs, I. E.; Jehng, J.-M.; Roberts, J. E. *Catal. Today* **1996**, *28*, 275.

10.1021/cm0477568 CCC: $30.25
Published on Web 04/22/2005

spectroscopic characterization and thermal transformation to VPO_4 in nitrogen via an internal oxidation−reduction reaction.

Experimental Section

Synthesis. Vanadium phosphorus oxide precursors were prepared as follows. Typically, vanadium pentoxide, V_2O_5 (3.0 g, 99%, Aldrich), and phosphorous acid, H_3PO_3 (3.5 g, 99%, Aldrich), were reacted with a mixture (60 mL) of 1-propanol and distilled water with various water concentrations (0, 8.3, 16.7, 50 vol %) in an autoclave at 150 °C for 24 h. Prior to reaction, the air in the autoclave was replaced with N_2. The solid was recovered by filtration, washed with acetone, and dried at 110 °C in air for 24 h. The samples prepared with different water content were denoted VPO-0, VPO-1, VPO-2, and VPO-3, respectively.

Characterization. Powder X-ray diffraction patterns were recorded with an Enraf-Nonius FR590 diffractometer using a Cu Kα source fitted with an Inel CPS 120 position sensitive detector. Laser Raman spectra were obtained with a Renishaw Ramanscope spectrograph fitted a green Ar^+ laser using ca. 25 mW of the 514.532 nm line for excitation. Infrared spectra were recorded on Nicolet 730 FTIR spectrometer using the KBr disk technique. Thermogravimetric analysis was performed using a Perkin-Elmer TGA instrument. The sample was heated from 30 to 800 °C in N_2 at a rate of 10 °C/min. The surface area was measured by a BET method with a using a Micromeritics automatic adsorption system.

Elemental analysis of the samples for C and H was performed using a CHN analyzer. The contents of V and P were determined by an inductively coupled plasma atomic emission spectrometer (ICP-AES, model Atom Scan 16, TJA Corp.), in which the sample powder was dissolved into hot H_2SO_4 and solution was diluted with water to about 30 ppm of V and P. The content of oxygen in the sample was calculated by subtracting the sum of weights of V, P, C, and H.

In situ XRD experiments were performed with an Enraf-Nonius FR590 diffractometer equipped with an in situ cell using a Cu Kα source fitted with an Inel CPS 120 position sensitive detector. The working voltage and current were 100 mA and 40 kV. Reactant gases were fed to the in situ cell using calibrated mass flow controllers. The total volume flow rate was 60 mL/min for all the studies.

Catalyst Testing. The selective oxidation of *n*-butane was carried out using a stainless steel microreactor. *n*-Butane and air were fed to the reactor via calibrated mass flow controllers to give a feedstock composition of 1.5% *n*-butane in air, and a total feed gas space velocity of 1700 mL gas/ml catalysts/h was employed. The products were analyzed by on-line gas chromatography. Carbon mass balances of ≥97% were typically observed. The catalyst precursors were heated in situ (1.5% *n*-butane in air) to the reaction temperature from room temperature at a rate of 3 °C/min.

Results and Discussion

Synthesis and Characterization of $VOHPO_3 \cdot 1.5H_2O$. In a previous study, Guliants et al.[7] prepared $VOHPO_3 \cdot 1.5H_2O$ using a method in which vanadium pentoxide was refluxed in anhydrous ethanol for 16 h to reduce V(V) to V(IV) and then phosphorous acid was added to give a P/V ratio of 1.0−1.3 and the reaction mixture was refluxed for another 20 h. The material synthesized as a powder has a surface area of 13−20 m^2/g. This vanadyl phosphite could be transformed into vanadyl pyrophosphate catalysts with high surface area (ca. 45 m^2/g) by online activation with *n*-butane/air in an activation procedure similar to the well documented one for $VOHPO_4 \cdot 0.5H_2O$.[13,17] The vanadyl pyrohosphate derived from this process showed high selectivity to maleic anhydride in *n*-butane partial oxidation comparable to the conventional unpromoted catalysts.[7,8]

Table 1. Elemental Composition and BET Surface Area of Vanadium Phosphorus Oxides

	VPO-0	VPO-1	VPO-2	VPO-3
V, wt %[a]	30.50 (1.00)	29.58 (1.00)	29.62 (1.00)	29.95 (1.00)
P, wt %[a]	19.94 (1.06)	19.82 (1.10)	19.64 (1.08)	19.56 (1.05)
C, wt %[a]	5.01 (0.69)	0.60 (0.09)	0.24 (0.03)	0.13 (0.02)
H, wt %[a]	2.55 (4.25)	1.82 (3.14)	1.74 (3.00)	1.72 (2.92)
O, wt %[a]	42.00 (4.38)	48.18 (5.19)	48.76 (5.26)	48.64 (5.15)
surf area (m^2/g)	51.4	8.5	3.2	0.5

[a] The values in the parentheses are relative atomic ratios.

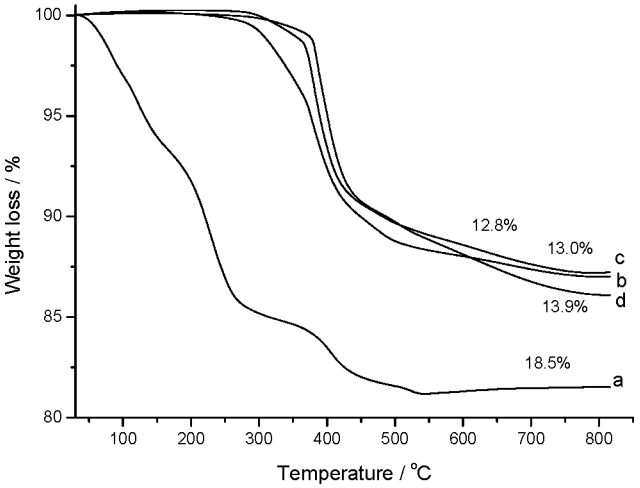

Figure 1. TGA curves of vanadyl hydrogen phosphite hydrates in N_2. Heating rate: 10 °C/min.

In this study, vanadium pentoxide was reacted with phosphorous acid and 1-propanol in an autoclave at a higher temperature of 150 °C for 24 h. The resulting product of VPO-0 was characterized by a combination of various characterization methods such as elemental analysis, BET, TGA, XRD, laser Raman spectra, and FT-IR, and the corresponding results are shown in Table 1 and Figures 1−4, respectively. The elemental analysis indicates that the composition of VPO-0 is $VPC_{0.7}H_{4.3}O_{4.4}$. TGA of VPO-0 shows multistep weight losses at 100, 230, 400, and 525 °C, in which the weight loss below 300 °C corresponds to the loss of structural and intercalated water whereas above 300 °C it is considered that the weight loss can be attributed to a loss of alcohol residues trapped in the particle agglomerates in the resultant product. The total weight loss observed is 18.5%, higher than the value of weight loss of 13.8% for the stoichiometric conversion of $VPC_{0.7}H_{4.3}O_{4.4}$ to VPO_4. This is mainly due to two factors. First it is possible that, in addition to water, volatile phosphorus and esters or other species were also formed and this contributed to the difference observed. Second, there was a difference in the pretreatment conditions of VPO-0 sample for elemental analysis and TG analysis; i.e., the VPO-0 for elemental analysis was dried at 100 °C in air overnight, whereas the

(17) Hutchings, G. J.; Desmartin Chomel, A.; Olier, R.; Volta, J. C. *Nature* **1994**, *368*, 41.

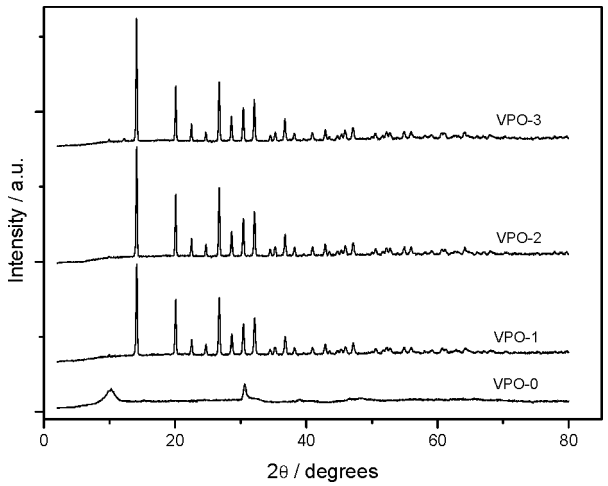

Figure 2. Powder XRD patterns of vanadyl hydrogen phosphite hydrates.

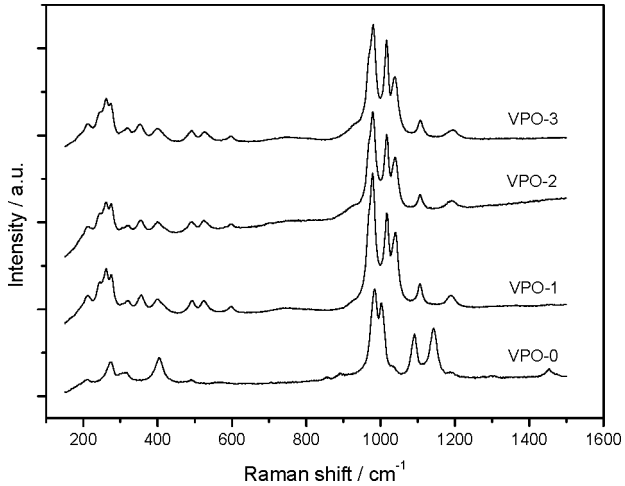

Figure 3. Laser Raman spectra of vanadyl hydrogen phosphite hydrates.

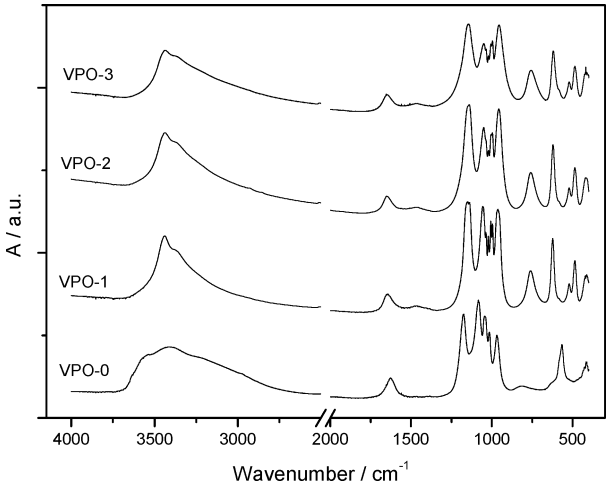

Figure 4. FT-IR spectra of vanadyl hydrogen phosphite hydrates.

sample for TG analysis was not pretreated prior to analysis and this may have introduced the variance in the two observations. This may also explain why the composition of VPO-0 is not consistent with $VOHPO_3 \cdot 1.5H_2O$ although powder X-ray diffraction (Figure 1), laser Raman (Figure 2), and IR spectra (Figure 3) confirm that they have essentially the same structure. On the other hand, the present results further confirm that the intercalated and structural water in the phosphite is involved in a weak interlayer bonding interaction with vanadyl groups. The weak interlayer interactions are key to the facile removal of the water,[8] and this is in contrast with the structural water in $VOHPO_4 \cdot 0.5H_2O$, wherein water forms strong hydrogen bonds with the P−OH groups in adjacent layers.

Table 2. Raman and IR Peaks of the VPO-0 Sample at Room Temperature[a]

Raman (cm^{-1})	1454 W, 1143 M,1092 M, 1033 W, 1002 vS, 984 vS, 892 vW, 491 vW, 405 M, 310 W, 273 M, 209 W
IR (cm^{-1})	3536 S, 3412 S br, 3228 S, 2968 sh, 2440 W, 1626 W, 1174 vS, 1082 vS, 1042 vS, 1014 S, 968 S, 817 W, 630 sh br, 566 S, 412 M

[a] Labels: vS = very strong; S = strong; M = medium; W = weak; sh = shoulder; br = broad.

XRD results indicate the interlayer spacing of VPO-0 is larger than that previously reported for $VOHPO_3 \cdot 1.5H_2O$ (8.59 vs 7.27 Å). This difference is probably due, among other factors, to the structure of vanadyl phosphite being strongly dependent on the nature of the solvent used during its crystallization, as indicated earlier by Guliants et al.[7] The Raman spectrum of VPO-0 is shown in Figure 3, and Table 2 summarizes the Raman shift of the bands. The Raman spectrum of VPO-0 exhibits the same features as that of $VOHPO_3 \cdot 1.5H_2O$. The bands at 1143 and 1092 cm^{-1} correspond to symmetric and asymmetric V−O−P stretching modes. The band at 1033 cm^{-1} corresponds to the P−H stretching mode. The band at 1002 cm^{-1} was tentatively assigned to a V═O stretching mode previously by Guliants et al.[7] The strong band at 984 cm^{-1} is assigned to symmetric P−O stretching mode, whereas the coupled V−O and P−O bending modes are observed in the 400−600 cm^{-1} range. Below 300 cm^{-1} the bands correspond to skeletal vibration of VO_6 and HPO_3 groups. The infrared spectrum of VPO-0 is shown in Figure 4a. The wavenumbers of the IR bands are listed in Table 2. VPO-0 exhibits a number of similar features in the IR spectrum with $VOHPO_3 \cdot 1.5H_2O$, i.e., the strong and broad features at ca. 3600−2800 cm^{-1} due to coordinated water, a band at 2440 cm^{-1} due to P−H linkages, and a number of symmetric and antisymmetric P−O stretching modes in the range of 1300−850 cm^{-1}, as well as P−O bending modes below 700 cm^{-1}. The above results clearly confirm that VPO-0 has essentially the same structure as reported for $VOHPO_3 \cdot 1.5H_2O$.[7]

It is possible that some other vanadium phosphates could also be formed during the autoclave preparation step because phosphorous acid is a well-known reducing agent for V(V) which oxidizes it into orthophosphate. As a result, both $VOHPO_4 \cdot 0.5H_2O$ and $VOPO_4 \cdot 2H_2O$ may be expected as impurities in the synthesis of vanadyl phosphite according to the following reactions:

$$V_2O_5 + H_3PO_3 = 2VO_2 + H_3PO_4$$

$$VO_2 + H_3PO_4 = VOHPO_4 \cdot 0.5H_2O + 0.5H_2O$$

$$V_2O_5 + 2H_3PO_4 + H_2O = VOPO_4 \cdot 2H_2O$$

Although the reaction was conducted in the absence of water, the complete removal of water from the reaction mixture is impossible as the alcohol is oxidized to an

aldehyde or ketone (during the reduction of V(V) to V(IV)) and these can produce water via aldol condensations. Water can also be formed by the direct reduction of V_2O_5 by alcohols:

$$V_2O_5 + 2ROH = V_2O_4 + R_2O + H_2O$$

Hence, there are many routes for the formation of water in the reaction. However, close inspection of the laser Raman and IR spectra does not reveal the presence of $VOPO_4 \cdot 2H_2O$ or $VOHPO_4 \cdot 0.5H_2O$ as there are no Raman bands at 952 ($\nu_s(PO_4^{3-})$) or at 542 ($\delta(PO_4^{3-})$) cm^{-1} or an IR band at 680 ($\omega(H_2O)$) cm^{-1} due to $VOPO_4 \cdot 2H_2O$ as well as IR bands at 1195, 1103, and 1050 (assigned to $\nu_s(PO_3)$), 1131 ($\delta_{ip}(POH)$), 930 ($\nu(P-OH)$), 641 ($\delta_{oop}(POH)$), and 535 and 484 ($\delta(OPO)$) cm^{-1} due to $VOHPO_4 \cdot 0.5H_2O$.[14,16,18] In addition, during experiments we found the $VOHPO_3 \cdot 1.5H_2O$, VPO-0, prepared in pure 1-propanol freely dissolved in hot water to form a light blue solution, which further excludes the possibility of the formation of $VOHPO_4 \cdot 0.5H_2O$ since $VOHPO_4 \cdot 0.5H_2O$ is not soluble in water and water is frequently used to purify the material.[18]

Synthesis and Characterization of $VOHPO_3 \cdot H_2O$. In the above study the reaction of vanadium pentoxide with phosphorous acid and 1-propanol in an autoclave at 150 °C led to the formation of $VOHPO_3 \cdot 1.5H_2O$ with an orthorhombic structure and V−P−O connectivity similar to $VOHPO_4 \cdot 0.5H_2O$ or $VOCH_3PO_3 \cdot 1.5H_2O$. Whereas, when water was added in the reactants, it was found that $VOHPO_3 \cdot H_2O$ was formed as the sole product. It is also possible that $VOHPO_3 \cdot 1.5H_2O$, $VOPO_4 \cdot 2H_2O$, and $VOHPO_4 \cdot 0.5H_2O$ could be formed as impurities. However, since $VOHPO_3 \cdot 1.5H_2O$ and $VOPO_4 \cdot 2H_2O$ are known to dissolve freely in hot water, to form a light blue colored solution and a light purple-red colored solution, respectively, the formation of $VOHPO_3 \cdot 1.5H_2O$ and $VOPO_4 \cdot 2H_2O$ as impurities was not considered possible in this study as the preparation incorporated water and the $VOHPO_3 \cdot 1.5H_2O$ and $VOPO_4 \cdot 2H_2O$ would not have precipitated but remained in the solution if they were formed during the preparation. To further confirm the hypothesis, VPO-1 sample was washed in hot water, and the filtrate was found colorless and transparent; analysis of filtrate confirmed the absence of V and P, which confirms that $VOHPO_3 \cdot 1.5H_2O$ and $VOPO_4 \cdot 2H_2O$ were not formed in the products. In addition the most intense reflection (*d* spacing of 5.719 Å) due to $VOHPO_4 \cdot 0.5H_2O$, a nonwater soluble phosphate, is absent in the XRD patterns of the VPO samples 1−3, which excludes the possibility of the formation of $VOHPO_4 \cdot 0.5H_2O$ in the products. The elemental analysis of the vanadyl hydrogen phosphite synthesized in a mixture of 1-propanol and water is summarized in Table 1. The results indicate that the compositions of VPO-1, VPO-2, and VPO-3 are consistent with vanadyl hydrogen phosphite monohydrate, $VOHPO_3 \cdot H_2O$. BET surface area measurements reveal that, with increasing water content in the solution, the surface area of resultant vanadyl hydrogen phosphite hydrates decreases significantly from the initial value of 51 m^2/g of VPO-0 to 0.5 m^2/g of VPO-3. TG curves show that these three vanadyl hydrogen phosphite monohydrates, VPO-1, VPO-2, and VPO-3, have a well-defined weight loss at around 400 °C and continuous loss up to the final temperature of 800 °C. The weight losses for these three samples are 13.0, 12.8, and 13.9%, respectively. For the stoichiometric conversion of $VOHPO_3 \cdot H_2O$ to VPO_4 a weight loss of 11.5% is expected which is less than the observed values. The differences observed are probably due to excess water adsorbed onto the powder samples.

(18) Hutchings, G. J.; Higgins, R. (Imperial Chemical Industries). U.K. Patent 1601121, 1981.

Table 3. Raman and IR Peaks of $VOHPO_3 \cdot H_2O$ at Room Temperature[a]

Raman (cm^{-1})	1192 W, 1106 W, 1038 S sh, 1016 vS, 979 vS, 598 W, 527 W, 492 W, 403 W, 352 W, 317 W, 276 sh, 260 S, 241 sh, 211W
IR (cm^{-1})	3436 S br, 3367 sh, 2478 W, 1649 W, 1140 vS, 1050 vS, 1021 w, 996S, 956 vS, 758 M, 621 S, 521 W, 484 M, 419 M

[a] Labels: vS = very strong; S = strong; M = medium; W = weak; sh = shoulder; br = broad.

Powder XRD patterns of VPO-1, VPO-2, and VPO-3 are also shown in Figure 2. The XRD patterns of the samples show rather similar features and can be fully indexed to $VOHPO_3 \cdot H_2O$ with a body-centered tetragonal structure, which is in agreement with the results of elemental analysis.

Raman spectroscopy has been widely recognized as a very sensitive characterization technique for metal oxide and phosphates. It may also be useful in establishing local structural differences in analogous compounds. The Raman and IR spectra of $VOHPO_3 \cdot H_2O$ have not been reported previously.[9] Thus, detailed Raman spectroscopy studies of these vanadyl hydrogen phosphite monohydrates were carried out. The main Raman bands of vanadyl hydrogen phosphite monohydrate exhibit a number of common features, including V−O−P stretches between 1000 and 1200 cm^{-1}, coupled V−O and P−O bending modes, and skeletal vibrations between 150 and 600 cm^{-1}. The Raman bands of $VOHPO_3 \cdot 1.5H_2O$ at 1143 and 1092 cm^{-1} corresponding to a V−O−P stretch are shifted to 1192 and 1106 cm^{-1} in $VOHPO_3 \cdot H_2O$, indicating a larger bond angle of V−O−P in the latter material because the V−O−P stretch is related to the V−O−P bond angle: the larger the bond angle, the higher the frequency of the Raman band.[14] The band at 1038 cm^{-1} probably corresponds to the P−H stretching mode, which appears at 1042 cm^{-1} in laser Raman spectrum of $VOHPO_3 \cdot 1.5H_2O$. The band at 1016 cm^{-1} is tentatively assigned to the V═O stretching mode which is expected to be in the 990−1000 cm^{-1} range on the basis of the average V═O bond length of all vanadium phosphates known to be similar (1.57−1.58 Å).[14] The band at 979 cm^{-1} in the Raman spectrum of $VOHPO_3 \cdot H_2O$ (Figure 3 and Table 3) could be assigned to another symmetric P−O stretching mode, whereas the coupled V−O and P−O bending modes are observed in 400−600 cm^{-1} range. Below 300 cm^{-1} the bands correspond to skeletal vibrations of VO_6 and HPO_3 groups.

The infrared spectrum of $VOHPO_3 \cdot H_2O$ (Figure 4 and Table 3) exhibits a band at ca. 3370 cm^{-1}, corresponding to the stretching mode for coordinated water. The weak band at ca. 1626 cm^{-1} may be assigned to the bending mode of water molecules. The band at 2440 cm^{-1} in the spectrum of

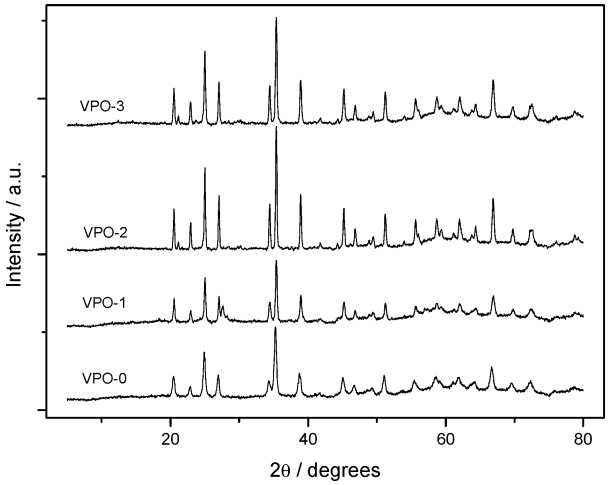

Figure 5. Powder XRD patterns of vanadyl hydrogen phosphite hydrates samples after the thermal treatment in N_2 at 750 °C.

$VOHPO_3 \cdot 1.5H_2O$ indicates P−H linkages in the structure,[7] which is shifted to 2478 cm^{-1} in the spectrum of $VOHPO_3 \cdot H_2O$, suggesting short P−H band linkages. A number of symmetric and antisymmetric P−O stretching modes are observed in 1300−850 cm^{-1} ranges. Below 700 cm^{-1} the bands correspond to P−O bending modes.[7]

Structural Transformation of the Vanadyl Hydrogen Phosphite Hydrates. Phase transformations were observed when the as-synthesized VPO materials were treated in nitrogen at 750 °C for 6 h as shown in Figure 5. It is worth noting that all the samples were transformed into VPO_4 as the sole product. VPO_4 is one of the isostructural $CrVO_4$-type magnetic oxides, i.e., $TiPO_4$, VPO_4, β-$CrPO_4$, and $FePO_4$-II, sulfates $MnSO_4$ and $FeSO_4$, and vanadates $CrVO_4$ and $FeVO_4$-II. In these compounds, octahedra MO_6 (M = Ti, V, Cr, Mn, Fe, Ni) form linear chain along the *c* axis by sharing edge, and these chains are separated each other by tetrahedron $M'O_4$ (M′ = P, S, V). These $CrVO_4$-type oxides exhibit a wide spectrum of magnetic properties despite their structural similarity and have been studied over the past 50 years.[20,21] The conventional method for the preparation of VPO_4 either involves the reaction of $(NH_4)_2HPO_4$ and NH_4VO_3 at 950 °C in argon atmosphere for several hours, the reduction of α-$VOPO_4$ or $(VO)_2P_2O_7$ in a controlled high-purity hydrogen atmosphere, or the microwave-assisted selective deoxygenation of α-$VOPO_4 \cdot 2H_2O$ using graphitic carbon as a reducing agent.[21−23] This study provides a novel route for the preparation of VPO_4 material, which has been shown to be a potential electrode material for a novel sodium-ion or lithium-ion cell based on C/$NaVPO_4F$ or C/$LiVPO_4$.[24,25]

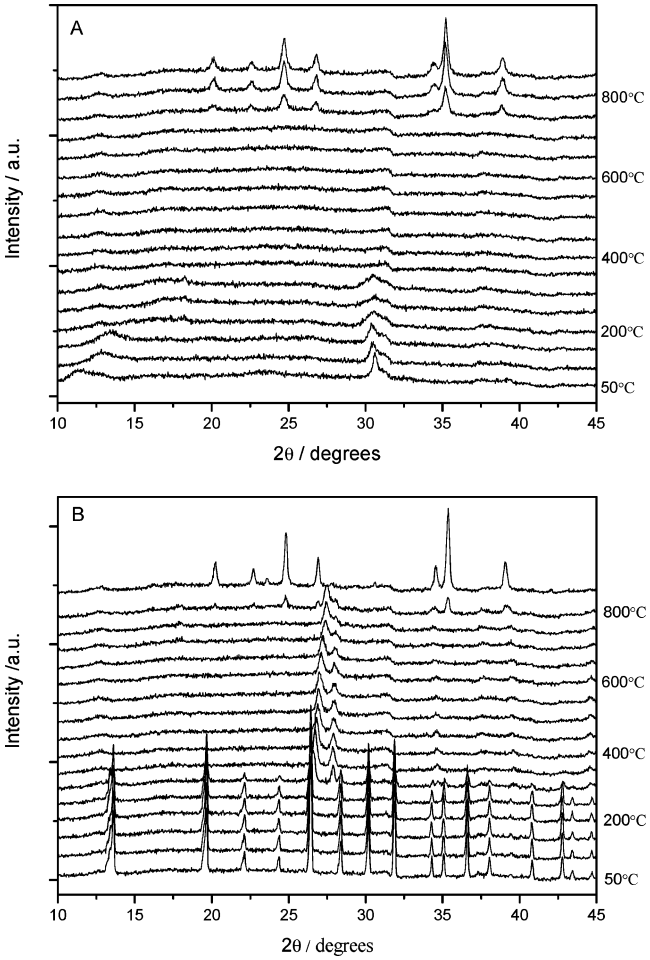

Figure 6. In situ powder XRD patterns of vanadyl hydrogen phosphite hydrates: (A) VPO-0; (B) VPO-2, during the thermal treatment in N_2 with increasing temperature. (The initial temperature was 50 °C, and patterns were taken at 50 °C intervals.)

To achieve a better understanding of this phase transformation process, the phase evolution of VPO-0 and VPO-2 samples was examined by in situ XRD during heating in flowing nitrogen. The temperature was increased from 50 to 800 °C with a heating rate 5 °C/min, 50 °C/step, and was held at 800 °C for 1 h. The XRD patterns were recorded at each step. The results are presented in Figure 6. The reflection (d = 8.59) of VPO-0 in the XRD patterns shifts to larger 2θ, and the intensity gradually decreases with increasing temperature owing to the loss of structural and intercalated water; at 350 °C it transformed to an amorphous material, while at higher than 750 °C the sample transformed to well-crystallized VPO_4. For VPO-2, the phase evolution exhibits different characteristics during thermal treatment. The intensity of reflections due to $VOHPO_3 \cdot H_2O$ also decline gradually with increasing temperature. At 350 °C all the reflections due to $VOHPO_3 \cdot H_2O$ disappear, whereas some new reflections emerge, which could not be indexed to any known VPO compound. As the thermal treatment temperature increases further, the reflections shift to larger 2θ. At 800 °C some reflections due to VPO_4 appear, and with prolonged thermal treatment time well-crystallized VPO_4 was formed. These results indicate that the structural rearrangement and phase transformation could be only completed at high temperature, and during this process an internal oxida-

(19) Busca, G.; Cavani, F.; Centi, G.; Trifiro, F. *J. Catal.* **1986**, *99*, 400.
(20) Koo, H.-J.; Whangbo, M.-H. *Inorg. Chem.* **2003**, *42*, 5932.
(21) Kinomura, N.; Muto, F.; Koizumi, M. *J. Solid State Chem.* **1982**, *45*, 252.
(22) Sananes, M. T.; Tuel, A. *Solid State Nucl. Magn. Reson.* **1996**, *6*, 157.
(23) Vaidhyanathan, B.; Ganguli, M.; Rao, K. J. *J. Mater. Chem.* **1996**, *6*, 391.
(24) Barker, J.; Saidi, M. Y.; Swoyer, J. L. *Electrochem. Solid State Lett.* **2003**, *6*, A1.
(25) Barker, J.; Saidi, M. Y.; Swoyer, J. L. *J. Electrochem. Soc.* **2003**, *150*, A1394.

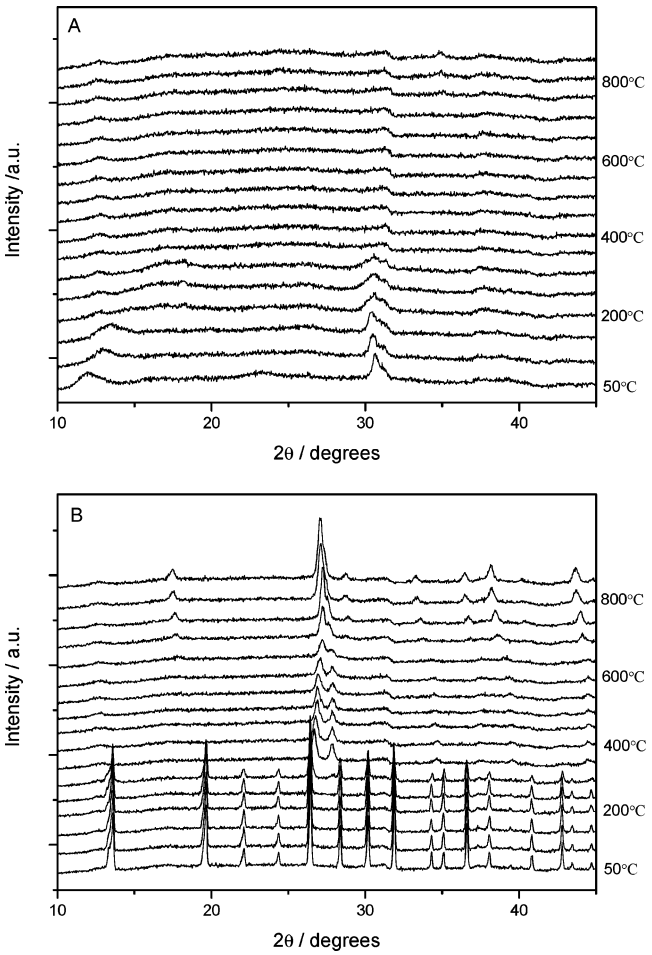

Figure 7. In situ powder XRD patterns of vanadyl hydrogen phosphite hydrates: (A) VPO-0; (B) VPO-2, during the thermal treatment in H_2 with increasing temperature. (The initial temperature was 50 °C, and patterns were taken at 50 °C intervals.)

tion−reduction reaction between V(IV) and P(III) occurred, wherein V(IV) was reduced to V(III) and P(III) was oxidized to P(V).

The phase evolution of VPO-0 and VPO-2 samples was also examined by in situ XRD during heating in flowing high-purity hydrogen to see whether hydrogen can suppress the internal oxidation−reduction reaction between V(IV) and P(III) in both vanadyl hydrogen phosphite hydrates and phase transformation from vanadyl hydrogen phosphite to VPO_4 as the phase transformation completes according to the following reactions:

$$2VOHPO_3{\cdot}1.5H_2O = 2VPO_4 + H_2 + 3H_2O$$

or

$$2VOHPO_3{\cdot}H_2O = 2VPO_4 + H_2 + 2H_2O$$

The results are presented in Figure 7. It is clear that below 700 °C the phase evolution of VPO-0 in flowing hydrogen shows trends similar to that in nitrogen. The reflection (d = 8.59) of VPO-0 in the XRD patterns shifts to larger 2θ, and the intensity decreases gradually with increasing temperature; at 350 °C it transformed to an amorphous material and remained amorphous until the final temperature of 800 °C. In the case of VPO-2, Figure 7b also reveals that below 700 °C the phase evolution of VPO-2 in hydrogen stream has

Table 4. Catalytic Performance of Vanadyl Hydrogen Phosphite Hydrates for the Oxidation of *n*-Butane to Maleic Anhydride[a]

catal	surf area (m^2/g) precursor	surf area (m^2/g) catal	reacn temp (°C)	conversion (%)	selectivity (%) MA	selectivity (%) CO	selectivity (%) CO_2	intrinsic activity/ 10^{-5} mol of MA m^{-2} h^{-1}
VPO-0	51	11	380	32	37	48	15	1.6
			400	37	41	44	15	2.1
VPO-2	3	4	380	20	39	48	13	2.6
			400	22	37	49	14	2.7
VPA[b]	1	1.5	400	4	45	25	30	1.9
VPO[b]	7	14	400	41	60	20	20	2.7

[a] Reaction conditions: 1.5 vol % *n*-butane in air; GHSV, 1700 h^{-1}. [b] Data from ref 28. GHSV = 2500 h^{-1}.

trends similar to that observed in nitrogen (Figure 6b). However, with a further increase in temperature surprisingly $V_2(PO_4)O$ with a V/P ration of 2 was formed which clearly indicates a loss of phosphorus occurs. Previously, VPO_4 was prepared by reduction of α-$VOPO_4$ in a controlled high-purity hydrogen atmosphere at high temperature[26] or $(VO)_2P_2O_7$ under 5% H_2 in argon using a linear increase of temperature from 25 to 900 °C,[22] suggesting that VPO_4 is difficult to reduce even at high temperature. Clearly, the present results confirm no VPO_4 phase formation upon heating both vanadyl hydrogen phosphite hydrates in flowing hydrogen at high temperature, and this is due to hydrogen inhibiting the phase transformation from vanadyl hydrogen phosphite to VPO_4 rather than the subsequent reduction of VPO_4.

Catalytic Performance of the Vanadyl Hydrogen Phosphite Hydrates. VPO-0 and VPO-2 samples were tested for the selective oxidation of *n*-butane, and the results are summarized in Table 4 and Figure 8. It is interesting to note that neither of these two catalysts requires an activation period to establish the steady-state catalytic performance which is generally associated with vanadium phosphate catalysts.[13,27] During this activation period, it is usual that catalysts derived from crystalline hemihydrate $VOHPO_4{\cdot}0.5H_2O$ undergo a structural transformation to $(VO)_2P_2O_7$ and $VOPO_4$ phases.[17] On the basis of activity/unit mass, samples VPO-0 and VPO-2 are not as effective as the reference vanadium phosphate based on $(VO)_2P_2O_7$. These further observations provide evidence that these materials are obviously different from the previously studied phosphate-based catalysts. The intrinsic activities for these catalysts, on the basis of the surface area determination after catalyst testing, are shown in Table 4. It is clear that the catalyst derived from VPO-2 ($VOHPO_3{\cdot}H_2O$) has a higher intrinsic activity for the production of maleic anhydride than that derived from VPO-0 ($VOHPO_3{\cdot}1.5H_2O$). The catalyst samples after testing were characterized by powder XRD and laser Raman spectroscopy. The results are presented in Figure 9. Both catalysts were found by XRD to be poorly crystalline, and only some weak reflections are observed in the XRD patterns. If one combines XRD with laser Raman spectroscopy, it is found that some crystalline $(VO)_2P_2O_7$, α_I-$VOPO_4$, and δ-$VOPO_4$ are present in both catalysts. However, the strong reflection at a d spacing of 3.27 Å in the

(26) Tudo, J.; Carton, D. *C. R. Acad. Sci. C* **1979**, *289*, 219.
(27) Hutchings, G. J.; Lopez-Sanchez, J. A.; Bartley, J. K.; Webster, J. M.; Burrows, A.; Kiely, C. J.; Carley, A. F.; Rhodes, C.; Hävecker, M.; Knop-Gericke, A.; Mayer, R. W.; Schlögl, R.; Volta, J. C.; Poliakoff, M. *J. Catal.* **2002**, *208*, 197.

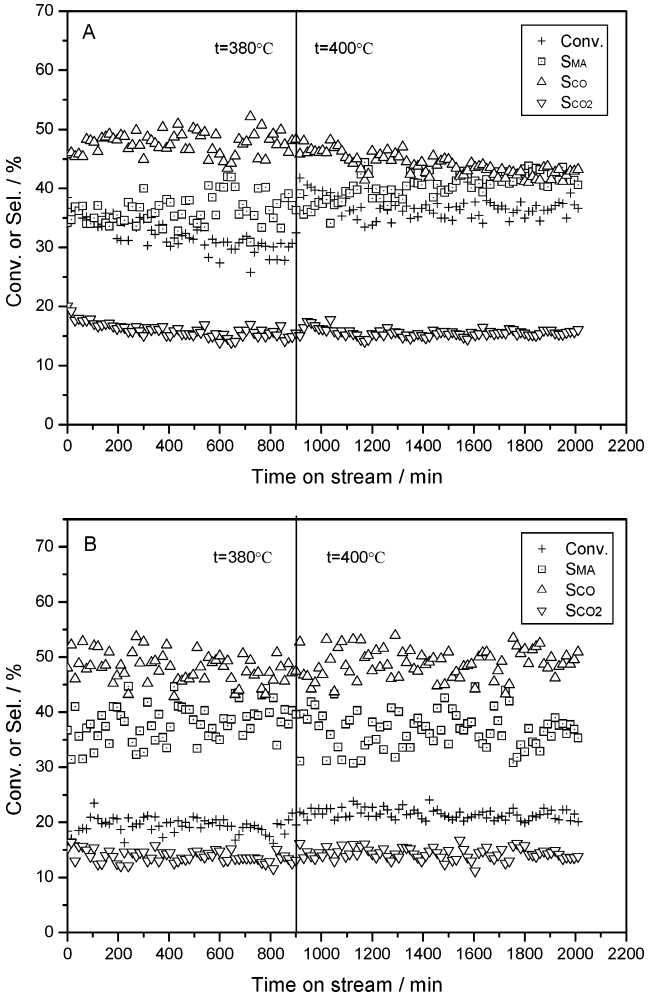

Figure 8. Catalytic performance of vanadyl hydrogen phosphite hydrates with time on stream: (A) VPO-0; (B) VPO-2.

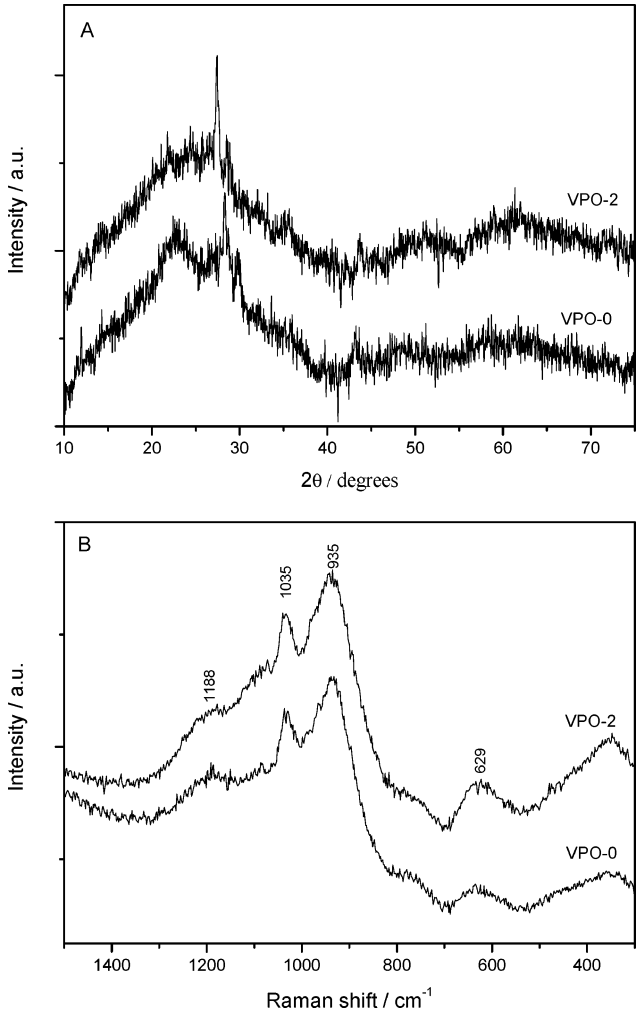

Figure 9. (A) Powder XRD patterns and (B) laser Raman spectra of the VPO catalysts after testing.

XRD pattern of the catalyst derived from the VPO-2 precursor could not be indexed to any known VPO compound. The vanadyl phosphite, VPO-0, prepared using the high-temperature one-pot method described in this study has a high surface area (ca. 50 m^2/g), which is much higher than those prepared by previous methods.[8] However, the catalyst derived from the VPO-0 precursor gave a lower BET surface area of 11 m^2/g than that reported in the previous study,[8] which is probably due to the difference of activation procedure. In the previous study reported by Guliants et al.,[8] $VOHPO_3 \cdot 1.5H_2O$ was activated in 1.2% *n*-butane in dry air at a space velocity of 400 h^{-1} in two steps: first at 320 °C for 1 day and then at 435 °C for 6 days. The catalyst obtained from that procedure showed the presence of only well-crystalline $(VO)_2P_2O_7$ and has a high surface area of ca. 40 m^2/g.[8] The differences suggest that $VOHPO_3 \cdot 1.5H_2O$ is very sensitive to the activation procedure, and to obtain well-crystalline vanadyl pyrophosphate with high surface area activation conditions should be chosen carefully. The activity and catalytic performance of the two samples VPO-0 and VPO-2 compare favorably with standard catalysts containing $(VO)_2P_2O_7$, α_{II}-$VOPO_4$, and δ-$VOPO_4$ prepared using aqueous (VPA) and nonaqueous methods (VPO).[28] The similarity of the intrinsic activities of maleic anhydride synthesis for VPO-0 and VPO-2 with the standard VPA and VPO materials confirm that the materials comprise poorly crystalline $(VO)_2P_2O_7$ and $VOPO_4$ phases, in contrast to those of the well-crystalline material in the study reported by Guliants et al.[8]

Conclusions

$VOHPO_3 \cdot 1.5H_2O$ with high surface area (ca. 50 m^2/g) was synthesized by reaction of V_2O_5, H_3PO_3, and 1-propanol in the absence of water at 150 °C in an autoclave, whereas in the presence of water $VOHPO_3 \cdot H_2O$ was found to be the unique product. On heating of the samples in flowing nitrogen at above 700 °C, the vanadyl(IV) hydrogen phosphite hydrates transformed into vanadium(III) phosphate, VPO_4, suggesting that during the structural rearrangement an oxidation−reduction process between V(IV) and P(III) occurred, wherein V(IV) was reduced to V(III) and P(III) was oxidized to P(V). Whereas, heating the vanadyl hydrogen phosphite hydrates in flowing hydrogen can inhibit the phase transformation from vanadyl hydrogen phosphite to VPO_4. The catalyst derived from the activation of $VOHPO_3 \cdot H_2O$ precursor shows the higher intrinsic activity for the selective

(28) Lopez-Sanchez, J. A.; Griesel, L.; Bartley, J. K.; Wells, R. P. K.; Liskowski, A.; Su, D.; Schlögl, R.; Volta, J. C.; Hutchings, G. J. *Phys. Chem. Chem. Phys.* **2003**, *5*, 3525.

oxidation of *n*-butane to maleic anhydride than that derived from $VOHPO_3 \cdot 1.5H_2O$, but both are similar to those derived from standard vanadium phosphate derived catalysts.

Acknowledgment. We thank Dr. Frank Girgsdies of the Fritz-Haber-Institüt der Max-Planck-Gesellschaft, Berlin, Germany, for indexing the powder X-ray pattern of $VOHPO_3 \cdot H_2O$. W.-S.D. is thankful for the financial support from Professor G. J. Hutchings and the Chinese Scholarship Council. Support from the EPSRC for this work is gratefully acknowledged.

CM0477568